PHOTOELECTRONICS

UDC 538.958 PACS: 81.15.Hi
EDN: KIJRKJ

Calculation of frequencies of mixed plasmon-phonon modes *p*-InSb and *p*-GaSb at *T* = 295 K

© A. G. Belov[1], E. V. Molodtsova[1], E. O. Zhuravlev[1], P. Yu. Kozlov[1], H. Yu. Komarovsky[1,2,*], A. N. Kuznetsov[3], H. A. Larionov[3]

[1] *Giredmet JSC, Moscow, 111524 Russia*
[*] *E-mail: nickkomarovskiy@mail.ru*
[2] *NUST MISIS, Moscow, 119049 Russia*
[3] *RD&P Center ORION, JSC, Moscow, 111538 Russia*

Received 22.01.2025; revised 21.02.2025; accepted 07.04.2025
Scientific specialty code: 2.2.3, 2.6.1

Theoretical calculations were carried out and values of light- and heavy-hole concentrations, as well as the effective mass of light holes, were derived for various values of the reduced Fermi level for p-InSb and p-GaSb at T = 295 K. The calculations took into account the non-parabolic nature of the light-hole band. The values of wave numbers corresponding to the plasma frequency, as well as the frequency of the high-frequency mixed plasmon-phonon mode, were calculated. Calibration curves were built to relate the concentrations of light and heavy holes to the characteristic wave number corresponding to the frequency of the high-frequency mixed plasmon-phonon mode. These curves were shown to be described by second-degree polynomials.

Keywords: p-type indium antimonide; *p*-type gallium antimonide; light and heavy holes; mixed plasmon-phonon modes; free carrier concentration.

DOI: 10.51368/1996-0948-2025-2-31-38

Introduction

Giredmet JSC has been working to create a contactless, non-destructive method for monitoring the free carrier concentrations (FCC) in various semiconductor materials for several years. The method is based on the analysis of infrared reflection spectra of heavily doped semiconductor samples and finding the concentration of free electrons or holes (depending on the conductivity type of the material). FCC is determined by the value of the characteristic wave number (ν_+) corresponding to the frequency of the high-frequency mixed plasmon-phonon mode.

The efforts taken have laid the groundwork and studied the samples of *n*-InSb [1], *n*-InAs [2], *n*-GaSb [3], *n*-GaAs [4, 5], *p*-GaAs [6], with the optical measurements compared to the Hall data obtained for the same samples [2–6]. This article continues an earlier series of works.

It will describe the algorithm developed for determining the concentrations of light and heavy holes in heavily doped *p*-InSb and *p*-GaSb at the room temperature.

The infrared reflection spectrum of the sample under study is recorded using any optical instrument in the wave number range of $\nu \leq 1500$ cm^{-1}. The derived spectral dependence of the reflectivity is processed according to the standard procedure using the Kramers-Kronig relations. The frequency dependences of the real, ε_1, and imaginary, ε_2, parts of the complex dielectric permittivity $\varepsilon = \varepsilon_1 + i\varepsilon_2$, after which the so-called "loss function" is constructed:

$$\mathrm{LF} = \mathrm{Im}\left(-\frac{1}{\varepsilon}\right) = \frac{\varepsilon_2}{\varepsilon_1^2 + \varepsilon_2^2}.$$

The wave numbers matching the maxima of the loss function correspond to the frequencies of mixed plasmon-phonon modes: ν_- – low-frequency one, and ν_+ – high-frequency one. It is only the high-frequency mode that will be of interest for us, since it is directly related to free charge carriers (the low-frequency mode is determined mainly by the crystal lattice of the material and is not suitable for determining the FCC value). By determining the value of ν_+ by means of the calculated calibration curves, one can calculate the concentration values of light and heavy holes. Building these curves is the goal of this paper.

All the calculations were made for $T = 295$ K. Results of the calculations given herein are assumed to be further used for comparing the optical and electrophysical measurements of hole concentrations in *p*-InSb and *p*-GaSb samples.

Theoretical calculations

The valence band of all A_3B_5 semiconductors is known to consist of two subbands (light and heavy holes) degenerated at point Γ of the Brillouin zone. Fig. 1 shows the band structures of InSb (*a*) [7] and GaSb (*b*) [8]. The heavy-hole bands for these materials are isotropic and parabolic. The light-hole bands are described by the Kane dispersion law [9], i.e. the effective mass of light holes increases as the energy grows.

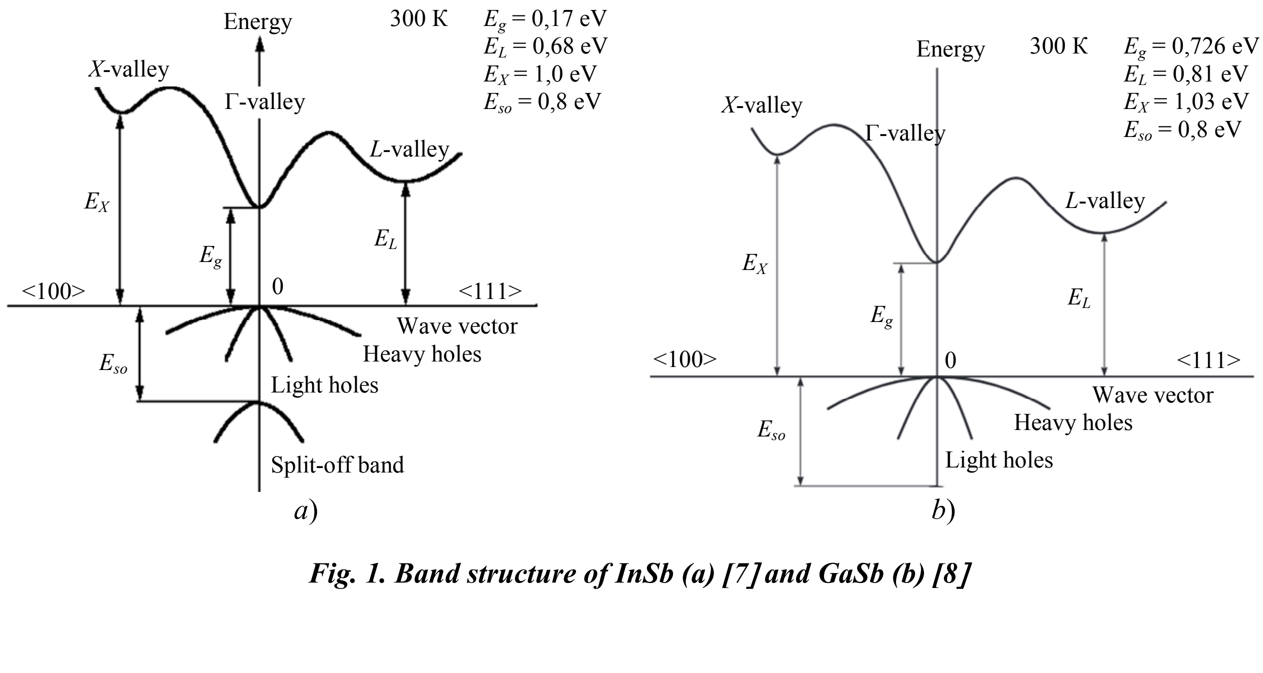

Fig. 1. Band structure of InSb (a) [7] and GaSb (b) [8]

When free charge carriers of two types are present, the plasma frequency is known to be written as [10]:

$$\omega_p^2 = \frac{4\pi e^2}{\varepsilon_\infty} \times \left(\frac{p_{\mathrm{H}}}{m_{p_{\mathrm{H}}}} + \frac{p_{\mathrm{L}}}{m_{p_{\mathrm{L}}}} \right) = \frac{4\pi e^2 p_{\mathrm{H}}}{\varepsilon_\infty m_{p_{\mathrm{H}}}} \times \left(1 + \frac{p_{\mathrm{L}} m_{p_{\mathrm{H}}}}{p_{\mathrm{H}} m_{p_{\mathrm{L}}}} \right). \quad (1)$$

Here p_{H}, p_{L} are concentrations of heavy and light holes, respectively; $m_{p_{\mathrm{H}}}$ and $m_{p_{\mathrm{L}}}$ are their optical effective masses; ε_∞ is the high-frequency dielectric permittivity; $e = 4.8\times10^{-10}$ units. CGSE – electron charge.

The second term in the brackets of formula (1) characterizes the contribution of light holes to the plasma frequency.

For the concentration of heavy holes (parabolic band) the relation [11] is true:

$$p_{\mathrm{H}} = \frac{8\pi}{3h^3} \times \left(2m_{p_{\mathrm{H}}} kT \right)^{\frac{3}{2}} \times F_{\frac{3}{2}}(\eta) \quad (2)$$

Here $F_{\frac{3}{2}}(\eta)$ is one-parameter Fermi integral:

$$F_{\frac{3}{2}}(\eta) = \int_0^\infty \left(-\frac{\partial f_0}{\partial x} \right) x^{\frac{3}{2}} dx, \quad (3)$$

where $f_0(x,\eta) = \left[1 + \exp(x-\eta) \right]^{-1}$; (4)

$\eta = \dfrac{E_F}{kT}$ is the reduced Fermi level (counted down from the top of the heavy-hole valence band – see Fig. 1).

The light-hole band is non-parabolic (Kane model [9]); in this case, the light-hole concentration is described by relation [11]:

$$p_{\mathrm{L}} = \frac{\sqrt{3}}{2\sqrt{2}\pi^2} \times \frac{\left(kTE_g \right)^{\frac{3}{2}}}{P_{cv}^3} \times {}^0L_0^{\frac{3}{2}}(\eta, \beta) \quad (5)$$

The effective mass of light holes can be calculated by formula [12, Appendix A]:

$$\frac{m_{p_{\mathrm{L}}}}{m_0} = \frac{3\hbar^2 E_g}{4P_{cv}^2 m_0} \times \frac{{}^0L_0^{\frac{3}{2}}(\eta, \beta)}{{}^0L_1^{\frac{3}{2}}(\eta, \beta)} \quad (6)$$

Here E_g is semiconductor's band gap; $k = 1.38\times10^{-16}$ erg/K is Boltzmann constant; (for $T = 295$ K $kT = 25.4$ meV); $\hbar = h/2\pi$, where $h = 6.62\times10^{-27}$ erg·s is Plank's constant; $m_0 = 9.11\times10^{-28}$ g is free-electron mass; $P_{cv} = 8.7\times10^{-8}$ eV·cm [13] is matrix element of interaction between the light-hole valence band and conduction band, considered to be the same for all compounds A_3B_5; $\beta = kT/E_g$ is parameter characterizing the non-parabolic nature of the light-hole band.

Formulas (5) and (6) use two-parameter Fermi integrals:

$${}^mL_k^n(\eta, \beta) = \int_0^\infty \left(-\frac{\partial f_0}{\partial x} \right) \frac{x^m \left(x + \beta x^2 \right)^n}{\left(1 + 2\beta x \right)^k} dx \quad (7)$$

The two-parameter integral ${}^0L_0^{\frac{3}{2}}(\eta, \beta)$ changes for a one-parameter integral $F_{\frac{3}{2}}(\eta)$ at $\beta \to 0$, the case when the non-parabolic nature of the band can be neglected.

Since the materials under consideration contain one heavy-hole band and one light-hole band, and both are isotropic, values of states density effective masses coincide with values of the optical effective masses – see formulas (1), (2), (5), (6).

Semiconductor materials A_3B_5 contain a noticeable proportion of ionic bond, therefore longitudinal optical vibrations of the crystal lattice (LO phonons) can interact with longitudinal collective vibrations of the system of free charge carriers – plasmons (plasmon-phonon coupling). This coupling shall be considered when building calibration curves relating the FCC values to the characteristic wave numbers.

If the damping of plasmons and LO phonons is neglected, the frequency dependence of the permittivity is written as:

$$\varepsilon(\omega)=\varepsilon_\infty\left[1-\left(\frac{\omega_p}{\omega}\right)^2\right]+\frac{\varepsilon_0-\varepsilon_\infty}{1-\left(\frac{\omega}{\omega_{LO}}\right)^2\times\frac{\varepsilon_0}{\varepsilon_\infty}}, \quad (8)$$

where ε_0 is static dielectric permittivity; ω is circular frequency; ω_{LO} is the frequency of the longitudinal optical phonon. The first term in formula (8) describes the plasmons' contribution, and the second term – the contribution from longitudinal optical phonons.

Longitudinal vibrations (which is what mixed plasmon-phonon modes are) are known to be able to exist in a medium only if the dielectric permittivity turns to zero. Accordingly, after equating expression (8) to zero and solving the biquadratic equation, thus switching from frequencies to wave numbers for ν_- and ν_+, we will have:

$$\nu_\pm^2 = \frac{1}{2}\left[\left(\nu_p^2+\nu_{LO}^2\right)\pm\sqrt{\left(\nu_p^2+\nu_{LO}^2\right)^2-4\frac{\varepsilon_\infty}{\varepsilon_0}\nu_p^2\nu_{LO}^2}\right] \quad (9)$$

Further only high-frequency mode ν_+ will be of interest for us.

The calculating algorithm is as follows:

– setting the value η and calculating the values p_H, p_L and $\frac{m_{p_L}}{m_0}$ by formulas (2), (5) and (6);

– substituting the derived values into formula (1) and calculating the value of plasma frequency ω_p and the corresponding wave number value: $\nu_p=\frac{\omega_p}{2\pi c}$, where $c = 3\times10^{10}$ cm/s is the speed of light in a vacuum;

– substituting the derived value of ν_p into formula (9) and calculating the value of ν_+;

– changing the value η and repeating the above steps;

– building calibration curves of the heavy- and light-hole concentrations vs. characteristic wave number: $p_H = f_1(\nu_+)$ and $p_L = f_2(\nu_+)$.

The following parameter values were used in the calculations:

for InSb:

$E_g = 0.17$ eV [7]; $\beta = 0.149$; $\varepsilon_0 = 18.0$, $\varepsilon_\infty = 15.68$ [13]; $m_{p_H} = 0.43\, m_0$; [7]; $\nu_{LO} = 197.2$ cm^{-1} [13];

for GaSb:

$E_g = 0.728$ eV [8]; $\beta = 0.0349$; $\varepsilon_0 = 16.4$, $\varepsilon_\infty = 15.2$ [13]; $m_{p_H} = 0.40\, m_0$; [8]; $\nu_{LO} = 240.3$ cm^{-1} [13].

Considering the above, formulas (2), (5) and (6) can be reduced to the following:

for InSb:

$$p_H = 5.185\times10^{18}\times F_{\frac{3}{2}}(\eta); \quad (10)$$

$$p_L = 2.676\times10^{16}\times {}^0L_0^{\frac{3}{2}}(\eta;\ 0.149) \quad (11)$$

$$\frac{m_{p_L}}{m_0}=0.0128\frac{{}^0L_0^{\frac{3}{2}}(\eta;\ 0.149)}{{}^0L_1^{\frac{3}{2}}(\eta;\ 0.149)}; \quad (12)$$

for GaSb:

$$p_H = 4.651\times10^{18}\times F_{\frac{3}{2}}(\eta);\qquad(13)$$

$$p_L = 2.376\times10^{17}\times{}^0L_0^{\frac{3}{2}}(\eta;\,0.0349)\qquad(14)$$

$$\frac{m_{p_L}}{m_0} = 0.0550\frac{{}^0L_0^{\frac{3}{2}}(\eta;\,0.0349)}{{}^0L_1^{\frac{3}{2}}(\eta;\,0.0349)}\qquad(15)$$

Formula (1) can be transformed as follows:

for InSb:

$$\nu_p = 1.152\times10^{-7}\times\sqrt{p_H\left(1+\frac{p_L m_{p_H}}{p_T m_{p_L}}\right)};\qquad(16)$$

for GaSb:

$$\nu_p = 1.213\times10^{-7}\times\sqrt{p_H\left(1+\frac{p_L m_{p_H}}{p_H m_{p_L}}\right)}\qquad(17)$$

Tables 1 and 2 present the parameter values calculated by the above formulas.

Table 1

Calculation results for p-InSb (T = 295 K)

η	p_H, cm^{-3}	p_L, cm^{-3}	$\frac{m_{p_L}}{m_0}$	ν_p, cm^{-1}	ν_+, cm^{-1}
-1.0	2.261×10^{18}	1.939×10^{16}	2.285×10^{-2}	186.6	224.1
-0.5	3.500×10^{18}	3.040×10^{16}	2.315×10^{-2}	232.2	253.9
0	5.273×10^{18}	4.664×10^{16}	2.359×10^{-2}	285.0	298.8
0.5	7.700×10^{18}	6.971×10^{16}	2.417×10^{-2}	344.4	354.2
1.0	10.863×10^{18}	10.124×10^{16}	2.492×10^{-2}	409.0	416.5
1.5	14.782×10^{18}	14.272×10^{16}	2.583×10^{-2}	477.1	483.2
2.0	19.464×10^{18}	19.555×10^{16}	2.690×10^{-2}	547.5	552.6
2.5	24.862×10^{18}	26.097×10^{16}	2.810×10^{-2}	618.8	623.2
3.0	30.934×10^{18}	34.017×10^{16}	2.941×10^{-2}	690.2	694.1

Table 2

Calculation results for p-GaSb (T = 295 K)

η	p_H, cm^{-3}	p_L, cm^{-3}	$\frac{m_{p_L}}{m_0}$	ν_p, cm^{-1}	ν_+, cm^{-1}
-1.0	2.028×10^{18}	1.188×10^{17}	6.513×10^{-2}	186.5	250.9
-0.5	3.139×10^{18}	1.839×10^{17}	6.535×10^{-2}	232.0	266.4
0	4.730×10^{18}	2.787×10^{17}	6.580×10^{-2}	284.7	302.1
0.5	6.907×10^{18}	4.098×10^{17}	6.635×10^{-2}	344.1	354.6
1.0	9.744×10^{18}	5.833×10^{17}	6.711×10^{-2}	408.7	416.1
1.5	13.260×10^{18}	8.028×10^{17}	6.802×10^{-2}	476.6	482.3
2.0	17.460×10^{18}	10.706×10^{17}	6.907×10^{-2}	546.8	551.5
2.5	22.301×10^{18}	17.530×10^{17}	7.158×10^{-2}	627.5	631.4
3.0	27.748×10^{18}	26.302×10^{17}	7.445×10^{-2}	708.1	711.4

As can be seen in Tables 1 and 2, the difference between the values of ν_p and ν_+ decreases as the hole concentrations increase, i.e. the influence of plasmon-phonon coupling weakens.

Using the data in Tables 1 and 2, one can built calibration curves relating hole concentrations to the characteristic wave number ν_+:

for InSb:

for heavy holes:

$$p_{\mathrm{H}} = 6.012\times10^{13}\times(\nu_+)^2 + 5.387\times10^{15}\times \times(\nu_+) - 1.814\times10^{18}; \quad (18)$$

for light holes:

$$p_{\mathrm{L}} = 9.628\times10^{11}\times(\nu_+)^2 - 2.136\times10^{14}\times \times(\nu_+) + 2.209\times10^{16}; \quad (19)$$

for GaSb:

for heavy holes:

$$p_{\mathrm{H}} = 3.246\times10^{13}\times(\nu_+)^2 + 2.390\times10^{16}\times \times(\nu_+) - 5.699\times10^{18}; \quad (20)$$

for light holes:

$$p_{\mathrm{L}} = 1.106\times10^{13}\times(\nu_+)^2 - 5.539\times10^{15}\times \times(\nu_+) + 8.965\times10^{16}. \quad (21)$$

All the calibration curves are described by second-degree polynomials.

Fig. 2 shows the calibration curves for heavy holes for *p*-InSb, *p*-GaAs and *p*-GaSb at $T = 295$ K for comparison purpose.

As can be seen in Fig. 2, the difference between the values of heavy-hole concentration for the listed semiconductor materials increases as the values of ν_+ increase.

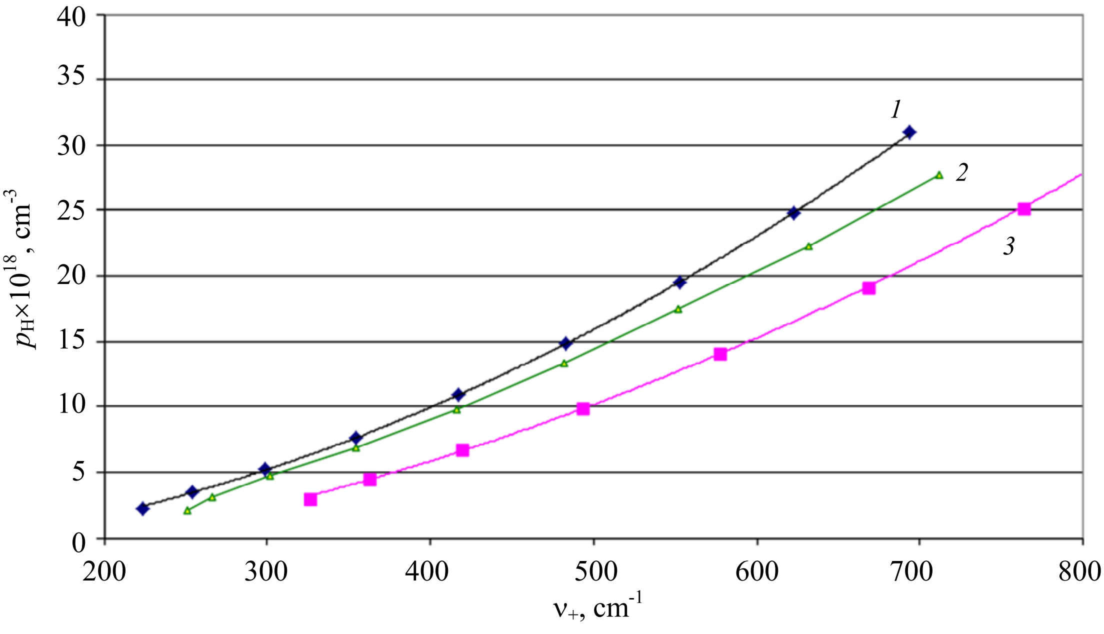

Fig. 2. Calculated calibration curves of the heavy-hole concentration: vs the characteristic wave number: curve 1 – p-Insb; curve 2 – p-GaSb; curve 3 – p-GaAs

The findings described in this paper are planned to be used for analyzing the data of optical and electrophysical measurements of *p*-InSb and *p*-GaSb samples. The same approaches were earlier used by us for *n*-GaSb [3] and *p*-GaAs [6] materials.

Conclusion

Calculations were carried out to derive the values of concentrations of light and heavy holes, effective mass of light holes, as well as frequencies of plasmons and mixed plasmon-phonon modes for *p*-InSb and *p*-GaSb at $T = 295$ K for various values of the reduced Fermi level. The calculations took into account the non-parabolic nature of the light-hole band.

Calibration curves were built to relate the concentrations of light and heavy holes to the characteristic wave number corresponding to the frequency of the high-frequency mixed plasmon-phonon mode. All the curves derived were shown to be described by second-degree polynomials.

REFERENCES

1. Belova I. M., Belov A. G., Kanevskiy V. E. and Lysenko A. P., Izvestiya vuzov. Elektronika **22** (3), 201–210 (2017). doi:10.214151/1561-5405-2017-22-3-201-210 [in Russian].

2. Yugova T. G., Belov A. G., Kanevskiy V. E., Kladova E. I., Knyazev S. N. and Parfent'eva I. B., Izvestiya vuzov. Materialy elektronnoy tekhniki **24** (3), 153–161 (2021). https://doi.org/10.17073/1609-3577-2021-3-153-161 [in Russian].

3. Belov A. G. Molodtsova E. V., Kormilitsina S. S., Kozlov R. Yu., Zhuravlev E. O., Klimin S. A., Novikova N. N. and Yakovlev V. A., Optika i spektroskopiya **131** (7), 919–925 (2023). doi: 10.21883/OS.2023.07.56126,4318-23 [in Russian].

4. Yugova T. G., Belov A. G., Kanevskij V. E., Kladova E. I. and Knyazev S. N., Izvestiya vuzov. Materialy elektronnoj tekhniki **23** (1), 27–33 (2020). doi: 10.17073/1609-3577-2020-1-27-33 [in Russian].

5. Komarovskiy N. Yu., Belov A. G., Kladova E. I., Knyazev S. N., Molodtsova E. V., Parfent'eva I. B. and Trofimov A. A., Applied Physics, № 6, 54–59 (2023). doi: 10.51368/1996-0948-2023-6-54-59 [in Russian].

6. Belov A. G., Kanevskiy V. E., Kladova E. I., Knyazev S. N., Komarovskiy N. Yu., Parfent'eva I. B. and Chernyshova E. V., Izvestiya vuzov. Materialy elektronnoy tekhniki **26** (3), 171–180 (2023). https://doi.org/10.17073/1609-3577j.met202304.525 [in Russian].

7. New semiconductor materials. Biology systems. Characteristic and properties. Band structure and carrier concentration of indium antimonide (InSb). URL https://www.ioffe.ru/SVA/NSM/Semicond/InSb/bandstr.html.

8. New semiconductor materials. Biology systems. Characteristic and properties. Band structure and carrier concentration of gallium antimonide (GaSb). URL https://www.ioffe.ru/SVA/NSM/Semicond/GaSb/bandstr.html.

9. Kane E. O., Journal of Physics and Chemistry of Solids **1** (4), 249–261 (1957). https://doi.org/10.1016/0022-3697(57)90013-6.

10. Pozhela Yu. K., Plazma i tokovye neustojchivosti v poluprovodnikah. Moscow, Nauka, 1977 [in Russian].

11. Askerov B. M., Kineticheskie effekty v poluprovodnikah. Moscow, Nauka, 1970 [in Russian].

12. Ravich Yu. I., Efimova B. A. and Smirnov I. A., Metody issledovaniya poluprovodnikov v primenenii k hal'kogenidam svintsa PbTe, PbSe, PbS. Moscow, Nauka, 1968 [in Russian].

13. Madelung O., Fizika poluprovodnikovyh soedineniy elementov III-V grupp; per. s angl. Moscow, Mir, 1967 [in Russian].

About authors

Alexander Georgievich Belov, Leading Research Assistant, Candidate of Physics and Mathematics, Giredmet JSC (111524, Russia, Moscow, Elektrodnaya Ulitsa, 2, bld 1). E-mail: IADenisov@rosatom.ru SPIN code 9546-0477, Author ID 38536

Elena Vladimirovna Molodtsova, Leading Research Assistant, Candidate of Technical Sciences, Giredmet JSC (111524, Russia, Moscow, Elektrodnaya Ulitsa, 2, bld 1). E-mail: evmol@bk.ru

Evgeny Olegovich Zhuravlev, Research Assistant, Giredmet JSC (111524, Russia, Moscow, Elektrodnaya Ulitsa, 2, bld 1).

Roman Yurievich Kozlov, Head of Laboratory, Giredmet JSC (111524, Russia, Moscow, Elektrodnaya Ulitsa, 2, bld 1). E-mail: RYKozlov@rosatom.ru

Nikita Yuryevich Komarovsky, Head of the research group, Giredmet JSC (111524, Russia, Moscow, Elektrodnaya Ulitsa, 2, bld 1), NUST MISIS (119049, Russia, Moscow, Leninsky Prospekt, 4, bld. 1). E-mail: nickkomarovskiy@mail.ru SPIN code 9642-8920, Author ID 1248206

Anton Nikolaevich Kuznetsov, Head of the Photonuclear Experiments Data Center, RD&P Center ORION, JSC (111538, Russia, Moscow, Kosinskaya Ulitsa, 9). E-mail: Kuznetsov.Ant.N@yandex.ru

Nikita Alexandrovich Larionov, Engineer Cat. 1, RD&P Center ORION, JSC (111538, Russia, Moscow, Kosinskaya Ulitsa, 9). E-mail: nikitalarionov16@yandex.ru SPIN code 1288-6349, Author ID 1242982